

# PHYSICS OBJECTIVES FOR FUTURE STUDIES OF THE SPIN STRUCTURE OF THE NUCLEON

WOLF-DIETER NOWAK

*DESY Zeuthen, Platanenallee 6, D-15738 Zeuthen, Germany*  
*e-mail: Wolf-Dieter.Nowak@desy.de*

**Abstract.** Physics perspectives are shown for future experiments in electron or positron scattering on nucleons, towards a deep and comprehensive understanding of the angular momentum structure of the nucleon in the context of Quantum Chromodynamics. Measurements of Generalised Parton Distributions in exclusive reactions and precise determinations of forward Parton Distributions in semi-inclusive deep inelastic scattering are identified as major physics topics. Requirements are discussed for a next generation of high-luminosity fixed-target experiments in the energy range 30-200 GeV.<sup>1</sup>

## 1. Introduction

Charged leptons have been used for more than two decades as a very powerful tool for studying the *momentum structure* of the nucleon, in a wide variety of experimental approaches. More recently, high-energy polarised beams and high-density polarised targets have become accessible and have proven to be indispensable tools in studying the *angular momentum structure* of the nucleon.

At large enough  $Q^2$ , the four-momentum-transfer squared of the photon mediating the lepton-nucleon interaction, short-range phenomena ('hard' photon-parton interactions) are successfully described by perturbative Quantum Chromodynamics (QCD). In contrast, long-range ('soft') phenomena and especially parton correlations in hadrons, over a broad range in  $Q^2$ , are still lacking a satisfactory theoretical description. Here it may be expected

<sup>1</sup>Invited talk at NATO 'Advanced Spin Physics Workshop', June 30-July 3, 2002, Nor-Hamberd, Armenia

that contemporary theoretical developments will at some point turn into a calculable field theoretical description of hadronic structures.

The spin of the nucleon as a whole is  $\frac{\hbar}{2}$ , irrespectively of the resolving power  $Q^2$  of the virtual photon. Due to angular momentum conservation in QCD the individual contributions of the parton's spins and orbital angular momenta always add up to this value, although they vary considerably with  $Q^2$ . Precise measurements at high and especially moderate  $Q^2$  are required to be able to reliably 'bridge' into the 'critical' region of  $Q^2 \leq 0.5 \text{ GeV}^2$  to eventually test theoretical descriptions of soft phenomena.

In this paper, based on recent theoretical developments in the field, an experimentalist's perspective is given on physics prospects for possible future electron-nucleon fixed-target experiments in the center-of-mass energy range of up to a few tens of  $\text{GeV}^2$ , with high resolution, high luminosity and polarised beams and/or targets.

## 2. Overview of the Relevant Quantities

The cross section of the inclusive reaction  $eN \rightarrow eX$  is not yet exactly calculable from theory. Instead it is presently parameterised by non-perturbative 'structure functions' which in turn, in the framework of the quark-gluon picture of the nucleon, are expressed in terms of Parton Distribution Functions (PDFs). These functions have proven to be very useful in the description of the momentum and spin structure of partons. However, they do not yet include the parton's *orbital* angular momenta which are considered to be essential among the various components that eventually make up the half-integer spin of the nucleon. This striking deficiency is cured in the formalism of 'Generalized Parton Distributions' (GPDs) [1, 2, 3, 4] which reached the level of practical applications only recently. This theoretical framework is capable of simultaneously treating several types of processes ranging from inclusive to hard exclusive scattering. Exclusive lepton-nucleon scattering is 'non-forward' in nature since the photon initiating the process is virtual and the final state particle is usually real, forcing a small but finite momentum transfer to the target nucleon. While it is very appealing that GPDs embody forward ('ordinary') PDFs as well as Nucleon Form Factors as limiting cases, they clearly contain a wealth of information well beyond these, notably about the hitherto unrevealed orbital angular momenta of partons (see below).

The scheme presented in Fig. 1 is intended as an easy-to-read overview of

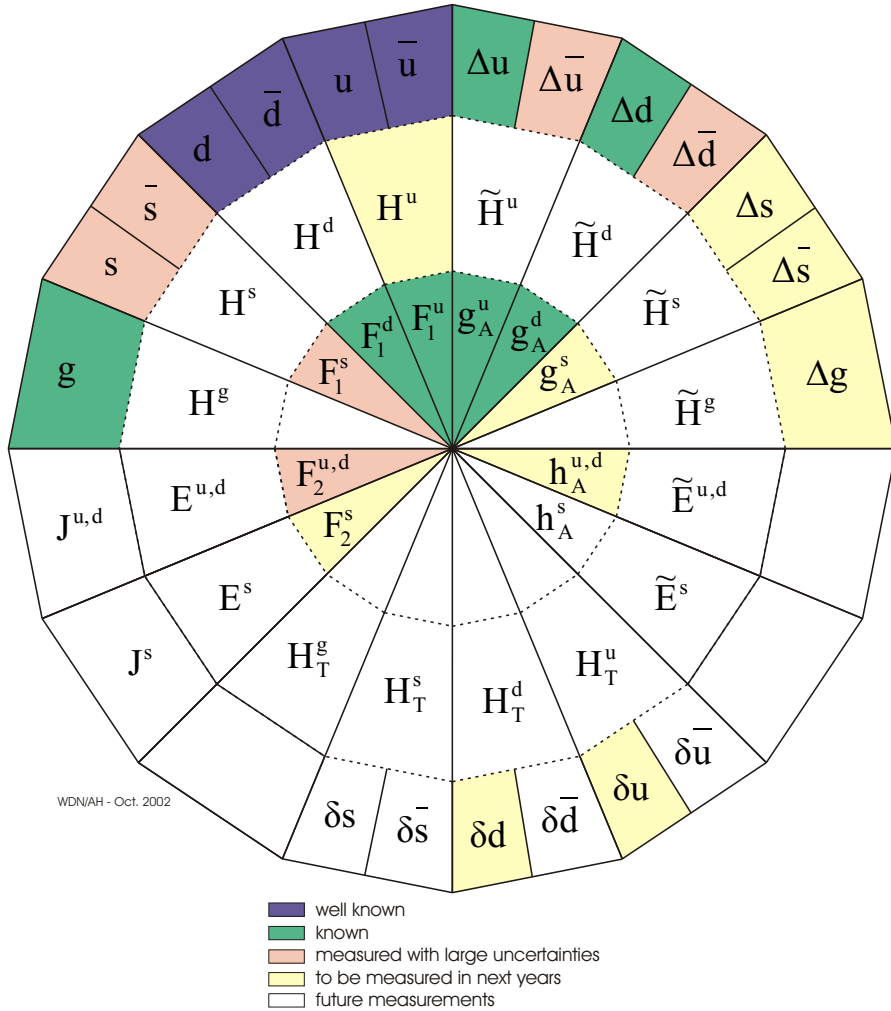


Figure 1. Visualisation of (most of) the relevant Generalised Parton Distributions and their limiting cases, forward Parton Distributions and Nucleon Form Factors. Different colours or shades of grey illustrate the status of their experimental access (see legend). For explanations see text.

the various quantities that are considered relevant for a comprehensive description of the angular momentum structure of the nucleon. It is based on the formalism of GPDs which are placed in the middle of three concentric rings. The two limiting cases are located in the adjacent rings: Nucleon Form Factors, the first moments of their appropriate GPDs, are shown in the innermost ring, while PDFs, their ‘forward’ limits, are located in the

outermost ring. Today’s experimental knowledge of the different functions is illustrated in different colours or shades of grey, from light (no data exist) to dark (well known), see legend. The emphasis in Fig. 1 is placed on the physics message and not on completeness; some GPDs have been omitted. Empty sectors mean that the function does not exist, decouples from observables in the forward limit, or no strategy is known for its measurement. GPDs will be discussed in detail in the next chapter, PDFs in chapter 4, and Nucleon Form Factors in chapter 5.

### 3. Generalized Parton Distributions

Generalized Parton Distributions depend on a resolution scale  $Q^2$ , two longitudinal momentum fractions ( $x, \xi$ ) and  $t$ , the momentum transfer at the nucleon vertex. The ‘skewedness’  $\xi$  parameterises the longitudinal momentum difference of the two partons involved in the interaction (cf. Fig. 2). Through their dependence on  $\xi$  the GPDs carry information about correlations between two different partons in the nucleon. Note that in the ‘forward’ limit  $\xi = 0$  and  $t = 0$ .

For each parton species<sup>2</sup>  $f$  there exist four GPDs ( $H^f, \tilde{H}^f, E^f, \tilde{E}^f$ ) that do not flip the *parton* helicity and additional four ( $H_T^f, \tilde{H}_T^f, E_T^f, \tilde{E}_T^f$ ) that do flip it [5, 6]. In terms of chirality the two sets of *quark* GPDs can be also referred to as chirally-even and chirally-odd ones, respectively, while gluons do not have chirality. The *nucleon* helicity, on the other hand, is conserved by the  $H$ -functions, but not by the  $E$ -functions. Finally, the chirally-even, i.e. parton-helicity non-flip quark GPDs can also be classified into unpolarised ( $H^f, E^f$ ) and polarised ( $\tilde{H}^f, \tilde{E}^f$ ) ones. The nucleon-helicity conserving quark GPDs  $H^f$  and  $\tilde{H}^f$  have as forward limits the well-known unpolarised and longitudinally polarised quark PDFs  $q_f, \bar{q}_f$  and  $\Delta q_f, \Delta \bar{q}_f$ , respectively. In the case of gluons,  $g$  and  $\Delta g$  are the forward limits of  $H^g$  and  $\tilde{H}^g$ , respectively. The nucleon-helicity non-conserving GPDs  $E^f$  and  $\tilde{E}^f$  decouple from observables in the forward limit, i.e. they have no corresponding PDFs. As forward limit of the *parton-helicity flip* quark GPDs  $H_T^f$  the transversity PDFs  $\delta q_f, \delta \bar{q}_f$  are obtained, while gluons have no transversity [7].

The recent strong interest in GPDs was stimulated by the finding [2] that the sum of the unpolarised chirally-even GPDs,  $\frac{1}{2}(H^f + E^f)$ , carries information about the *total* angular momentum  $J^f$  of the parton species  $f$

<sup>2</sup>Here  $f$  stands for the quark flavors  $u, d, s$ , but here also for the gluon index  $g$ .

in the nucleon. In the limit of vanishing  $t$  the second moment of this sum approaches  $J^f$ , measured at the given  $Q^2$ . The total angular momentum carried by quarks of all flavors,  $J^q = \sum_f J^f$ , and that carried by gluons,  $J^g$ , are not known yet. The same holds for the corresponding orbital momenta,  $L^q$  and  $L^g$ . Through the simple integral relation  $L^q = J^q - \frac{1}{2}\Delta\Sigma$ , with  $\frac{1}{2}\Delta\Sigma$  being the quark's *spin* contribution (cf. next chapter), a measurement of  $J^q$  would allow to determine  $L^q$ . Note that there is an ongoing unresolved controversy in the literature about the appropriate definition of angular momentum operators for quarks and gluons [8].

GPDs can in principle be revealed from measurements of various cross sections and spin asymmetries in several exclusive processes. However, there is no doubt that for a determination of individual GPDs from experimental cross sections and asymmetries a rather complicated procedure will have to be developed. Unlike in the case of forward PDFs a direct extraction of GPDs appears presently not feasible. The usual deconvolution procedure can not be applied, because the involved momentum fraction  $x$  is an entirely internal variable, i.e. it is always integrated over in the process amplitudes. A principal way to circumvent this problem by distinguishing the  $\log Q^2$  behaviour from the  $1/Q^2$  behaviour [9] appears hard to realise even under substantially improved experimental conditions in the future. Hence an iteration process based on the comparison of theoretical model GPDs to experimental data seems to be the unavoidable choice. This most probably will require the combination of results from various reaction channels into a ‘global fit’ of the involved GPDs. Clearly, further theoretical work on the sensitivity of experimentally available quantities to different properties of the model functions, especially higher orders (see e.g. Ref. [10]) and higher twists (see e.g. Ref. [11]), seems to be of great importance.

The chirally-even GPDs ( $H^f, \tilde{H}^f, E^f, \tilde{E}^f$ ) for  $u$  and  $d$ -quarks, which are presently the most intensely discussed functions, can be accessed experimentally in several reactions. Deeply Virtual Compton Scattering (DVCS),  $ep \rightarrow ep\gamma$  (cf. left panel of Fig. 2), is presently considered the cleanest one. In this reaction the first and, so far, the only GPD-related experimental results were published recently. Note that there is still no data available that can be related to parton-helicity non-flip *gluon* GPDs. They can in principle be accessed in DVCS and meson production at small  $\xi$ , i.e. preferentially at large center-of-mass energies.

A  $\sin \phi$  behaviour<sup>3</sup> is predicted [12] for the azimuthal dependence of the sin-

<sup>3</sup>Here  $\phi$  is the azimuthal angle of the produced real photon around the direction of the virtual photon, relative to the lepton scattering plane.

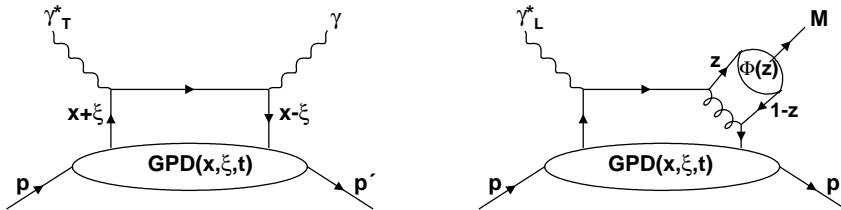


Figure 2. Illustration of the two major types of hard exclusive processes to extract GPDs: DVCS and Meson Production.

gle *beam-spin asymmetry* in the DVCS cross section. This prediction was recently proven at two different center-of-mass energies, by HERMES [13] and CLAS [14]. The asymmetry is given by the *imaginary* part of the interference term between the DVCS and Bethe-Heitler amplitudes. The involved combination of GPDs contains  $H^f$ ,  $\tilde{H}^f$  and  $E^f$ , where  $H^f$  is the dominant function driven by kinematical factors (cf. Ref. [15]). Access to the *real* part of the same interference term is opened by measuring the *beam-charge asymmetry* in DVCS. First results on this observable were presented by HERMES [16] very recently and confirmed the predicted  $\cos \phi$  behaviour. It has to be noted that the imaginary part is probed at the special argument  $(\xi, \xi, t)$  which constitutes a second independent ‘slice’ in the  $(x, \xi, t)$ -plane, in addition to the ‘forward slice’  $(x, 0, 0)$ . The  $x$ -dependence away from the line  $x = \xi$  is contained in the principal value integral of the real part [17].

Information on chirally-even GPDs can also be accessed in Deeply Virtual Exclusive production of pseudoscalar and vector Mesons (DVEM),  $ep \rightarrow epM$  (cf. right panel of Fig. 2). While DVCS is suppressed in comparison to meson production by the additional electromagnetic coupling, the latter is suppressed by a factor  $1/Q^2$  over the former. In fixed-target exclusive meson production, this results in an increase by a factor of about 10 in count rate, as compared to DVCS. On the other hand, compared to the outgoing real photon in DVCS the exclusively produced meson introduces one more complication, namely the distribution amplitude  $\Phi(z)$  as an additional unknown. Here  $z$  is the momentum fraction carried by the meson. Cross sections and spin asymmetries for different channels are described by different sets of GPDs (for more details see e.g. Ref. [17]). The comparison of pseudoscalar and vector meson production reveals that the final state meson acts in fact as a helicity filter. Fig. 3 illustrates which of the chirally-even GPDs can be accessed in which reaction channels.

Although there exists already a huge number of theoretical papers on

DVCS	$\gamma^* \mathbf{p} \longrightarrow \gamma \mathbf{p}$	$\mathbf{H} \quad \tilde{\mathbf{H}} \quad \mathbf{E} \quad \tilde{\mathbf{E}}$
exclusive pseudoscalar meson production	$\gamma^* \mathbf{p} \longrightarrow \pi^0 \mathbf{p}$	$\tilde{\mathbf{H}} \quad \tilde{\mathbf{E}}$
	$\gamma^* \mathbf{p} \longrightarrow \pi^+ \mathbf{n}$	
exclusive vector meson production	$\gamma^* \mathbf{p} \longrightarrow \rho^0 \mathbf{p}$	$\mathbf{H} \quad \mathbf{E}$
	$\gamma^* \mathbf{p} \longrightarrow \omega \mathbf{p}$	
	$\gamma^* \mathbf{p} \longrightarrow \phi \mathbf{p}$	

Figure 3. Examples of hard exclusive processes and the involved chirally-even GPDs.

chirally-even GPDs, only a few attempts have been made to construct models for them (cf. e.g. Ref. [17] and references therein, [18]). They have to reproduce the  $x$ -dependence of forward PDFs and the  $t$ -dependence known from Nucleon Form Factors. The crucial problem of the correlations between the different GPD variables is still under strong theoretical debate. It remains to be shown to which extent future experiments will be in a position to successfully distinguish between different GPD models. A very first glimpse of the function  $H$  can be expected to emerge from mid-term future measurements of various hard exclusive reactions, especially DVCS, at the HERMES experiment upgraded with a Recoil Detector [19] surrounding an *unpolarised* target. The projected measurements with an integrated luminosity of  $2 \text{ fb}^{-1}$  will be able to distinguish between two different sets of ‘contemporary’ model GPDs over a certain range in the longitudinal momentum variable  $\xi = x_B/(2-x_B)$ , where  $x_B$  is the Bjorken scaling variable. (For details see Refs. [15, 20]).

Considerably less theoretical work and no experimental results exist on either quark or gluon *helicity-flip* GPDs ( $H_T^f, \tilde{H}_T^f, E_T^f, \tilde{E}_T^f$ ). The first proposal how to experimentally access helicity-flip *quark* GPDs is based on the simultaneous production of two  $\rho$  mesons [21] at large rapidity separation. This may experimentally be feasible but requires large center-of-mass energies. No model has been proposed yet for these functions and therefore no projections are available yet. Helicity-flip *gluon* GPDs can in principle be accessed through measurements of a distinct angular dependence of the DVCS cross sections [5, 22].

As mentioned above, the forward limit of the second moment of the sum  $\frac{1}{2}(H^f + E^f)$  determines the total angular momentum  $J^f$  of the parton

species  $f$  in the nucleon. In this context a forward *orbital angular momentum (OAM) distribution* was introduced [23] as  $L^f(x) = J^f(x) - \Delta q_f(x)$ , where  $J^f(x)$  is the forward limit of the GPD sum  $\frac{1}{2}(H^f + E^f)$  and  $\Delta q_f(x)$  is the helicity distribution (cf. next chapter). Since the forward limit of the GPD  $H^f$  is known from the well-measured PDFs  $q_f$  and  $\bar{q}_f$ , a determination of  $J^f(x)$  requires a measurement of the GPD  $E^f$ . This is expressed in Fig. 1 by placing the symbol  $J^f$  in the outermost ring of the  $E^f$  sector. Experimental access to  $E^f$  may be achieved through DVCS measurements with an unpolarised beam and a *transversely* polarised target. Projections for the statistical accuracy attainable when measuring the relevant single target-spin asymmetry  $A_{UT}(\phi)$  are given in Ref. [29] for both a possible low-luminosity ( $0.8 \text{ fb}^{-1}$ ) measurement in the mid-term future and a high-luminosity measurement ( $100 \text{ fb}^{-1}$ ) in the far future. Note that the present HERMES measurements using a transversely polarised target, aiming at a determination of  $u$  and  $d$  quark transversity (cf. next chapter), are planned to collect about  $0.15 \text{ fb}^{-1}$ . Also, important additional knowledge on  $E^f$  can be expected from exclusive vector meson production with transverse target polarisation [17].

#### 4. Parton Distribution Functions

A Parton Distribution as forward limit of a Generalised Parton Distribution depends only on the constituent's momentum fraction  $x$  that in deep inelastic lepton-nucleon scattering (DIS) is identified with the Bjorken scaling variable  $x_B$ . Additionally, it depends on a resolution scale  $Q^2$ , as mentioned above. On the simplest (twist-2) level, as long as multi-parton correlations are not considered, the complete set of quark PDFs consists (for every flavor  $u, d, s$ ) of number density  $q_f$ , *longitudinally* polarised (helicity) distribution  $\Delta q_f$ , and *transversity* distribution  $\delta q_f$ . Only these three functions together form the minimum data set necessary for meaningful confrontations with theoretical models of the ground state of the nucleon.

In-depth studies of DIS over the last two decades resulted in unpolarised quark distributions that are precisely known for valence and well known for sea quarks [24]. Their longitudinally polarised counterparts were measured only recently [25], still with large uncertainties for the sea distributions. In contrast, the *transverse* spin structure of the nucleon is still completely unexplored, even in the forward limit. Several experiments will deliver first data in the near future: COMPASS at CERN [26], HERMES at DESY [27] and RHIC-spin at BNL [28]. Its interpretation will to a large extent be based on the analysis of (single) spin asymmetries in (semi-inclusive) hadron

production cross sections. However, precise information on sea quark as well as highly precise data on valence quark distributions can only be expected from the next generation of electron-nucleon scattering experiments. For a brief overview including projections and further references see, e.g., Ref. [29].

For a given flavor, the first moment of the sum (difference) of quark and anti-quark helicity (transversity) distributions represents the axial (tensor) charge of the nucleon. Precise measurements of these integrals are of special interest. The flavor sum of the axial charges,  $\Delta\Sigma(Q^2)$ , describes the quark's contribution to the total longitudinal spin of the nucleon. Experimentally, a value far below the originally expected non-relativistic limit is found, irrespectively of the underlying renormalisation scheme. This behaviour gave rise to the 'spin crisis' of the nineties. It may be attributed to the fact that the  $Q^2$ -evolution of  $\Delta\Sigma$  involves the polarised gluon distribution. In contrast, the hitherto totally unmeasured flavor sum of the tensor charges,  $\delta\Sigma(Q^2)$ , decouples as an all-valence object from gluons and sea quarks and hence is expected to be much closer to the non-relativistic limit (cf. the discussion on lattice QCD results below). Measurements of the tensor charge will give access to the hitherto unmeasured chirally-odd operators in QCD which are of great importance to understand the role of chiral symmetry in the structure of the nucleon [30]. Also, the tensor charge is required as input to calculate the electric dipole moment of the neutron [31] in beyond-the-standard-model theories where the quarks may have electrical dipole moments themselves [32].

Lattice calculations, performed in the context of the operator-product expansion (OPE), lead to reliable results on the 'valence' tensor charge  $\delta\Sigma \approx \delta u + \delta d$ ; their precision improves with time as better methods and computers are used (e.g.  $0.562 \pm 0.088$  in 1997 [33],  $0.746 \pm 0.047$  in 1999 [34]). Nevertheless, these values are far away from the non-relativistic limit of  $\frac{5}{3}$  expected for a nucleon consisting of just three valence quarks. In contrast, lattice OPE calculations do not yet lead to reliable results on the 'valence' axial charge  $\Delta\Sigma \approx \Delta u + \Delta d$ , because the quark-line disconnected diagram cannot be calculated yet. The 'quenched' approximation leads to the value  $\Delta\Sigma = 0.18 \pm 0.10$  [33]. This is surprisingly consistent with the earlier result  $0.18 \pm 0.02$  obtained with the simpler method of dynamically staggered fermions [35]. Note that next-to-leading order QCD analyses of experimental data yield  $\Delta\Sigma = 0.2 - 0.4$ , depending on the factorisation scheme [36]. All numbers quoted above refer to  $Q^2$ -values of a few  $\text{GeV}^2$ .

## 5. Elastic Form Factors

The  $t$ -dependent elastic form factors of the nucleon can in principle be obtained from the Generalised Parton Distributions (once they are known) by integrating over their momentum-fraction variables, i.e. as their first moments. The first moments of the unpolarised chirally-even GPDs  $H^f$  and  $E^f$  constitute the Dirac (charge) and Pauli (current) form factors  $F_1^f(t)$  and  $F_2^f(t)$ . Note that measurements are usually done for the electric and magnetic Sachs form factors  $G_E$  and  $G_M$  which are linear combinations of the Dirac and Pauli form factors. The polarised chirally-even GPDs  $\tilde{H}^f$  and  $\tilde{E}^f$  yield the axial-vector and pseudoscalar form factors  $g_A^f$  and  $h_A^f$  (also denoted as  $G_A$  and  $G_P$ ). Also for the helicity-flip quark GPDs ( $H_T^f, \tilde{H}_T^f, E_T^f, \tilde{E}_T^f$ ) form factors exist; for example the first moment of  $H_T^f$  at  $t = 0$  is the tensor charge of quark species  $f$ . The corresponding sectors in Fig. 1 contain no symbols because in the literature there is no unique naming convention nor are there ways for their measurement. For that reason the gluon form factors are also omitted.

Measurements of proton and neutron elastic form factors are accomplished by widely different experimental approaches. Beam energies of a few GeV and less are sufficient to determine their  $Q^2$ -dependence which can, in most cases, be approximately described by the  $1/Q^2$  dipole form factor. For a recent review of existing measurements and for further references, see Ref. [37].

## 6. Experimental Requirements

Presently, almost the entire field of GPD-related physics constitutes experimentally virgin territory. Stimulated by the physics insight that can be expected from measurements of GPDs, experimentalists are striving to optimise and upgrade their existing facilities to obtain experimental results that can be used to extract first information about GPDs themselves.

There is little doubt that a completely new step in experimentation, concerning both fixed-target and collider facilities, is required for future GPD measurements. In Fig. 4 a brief summary of the abovementioned major physics topics is given in conjunction with experimental requirements for a future fixed-target electron-nucleon scattering facility. It must offer luminosities of at least  $10^{35}$  per  $\text{cm}^2\text{s}$  requiring an accelerator with a duty cycle of 10% or more. Beam energies above 30 GeV are needed to cover a kinematic range suitable for extracting cross sections and their scale de-

pendence in exclusive measurements. For the non-exclusive studies of the hadron structure, including precise measurements of polarised Parton Distribution Functions, variable beam energies in the range of 50-200 GeV are required. In both cases, highest possible polarisation of beam and targets as well as the availability of both beam charges is required to fully exploit the potential of asymmetry measurements. Large-acceptance detector systems with high-rate capabilities must reach a mass resolution of a third of the pion mass, mandatory for the measurement of exclusive channels. For more detailed discussions of the various present-day options for such a facility see, e.g., Refs. [29, 38] which also contain further references. Note that precise measurements of Nucleon Form Factors, while constituting an essential part of the physics menu addressed in this paper, will be pursued at lower-energy facilities.

## 7. Conclusions

As can be concluded from today's knowledge, major steps in both theory and experimentation are required to accomplish a comprehensive understanding of the angular momentum structure of the nucleon. Physics objectives can be identified for a future fixed-target electron-nucleon scattering facility with polarised targets, high-luminosity, and variable beam energies of 30-200 GeV. Precise measurements of hard exclusive processes will have to be performed in several reaction channels towards a determination of as many as possible Generalised Parton Distributions in a 'global' fit. Independently, very precise measurements of the GPD limiting cases, namely forward Parton Distribution Functions on the one hand, and Nucleon Form Factors on the other, will be of great importance for further developments of the theory, because they eventually will have to complement and confirm the GPD results.

## Acknowledgements

I am deeply indebted to M. Diehl and X. Ji for enlightening discussions, to F. Ellinghaus, R. Kaiser and J. Volmer for a careful reading of the manuscript, and to K. Jansen and G. Schierholz for valuable comments on the lattice QCD section. Many thanks to B. Seitz for commenting on, and to A. Hagedorn for producing Fig. 1. The help of K. Pipke in preparing Fig. 4 is acknowledged.

## References

1. D. Müller *et al.*, Fortschr. Phys. **42**, 101 (1994).
2. X. Ji, Phys. Rev. Lett. **78**, 610 (1997); Phys. Rev. **D 55**, 7114 (1997).
3. A.V. Radyushkin, Phys. Lett. **B 380**, 417 (1996); Phys. Rev. **D 56**, 5524 (1997).
4. J. Blümlein *et al.*, Nucl. Phys. **B 560**, 283 (1999); Nucl. Phys. **B 581**, 449 (2000).
5. P. Hoodbhoy, X. Ji, Phys. Rev. **D 58**, 054006 (1998).
6. M. Diehl, Eur. Phys. J. **C 19** 485 (2001).
7. X. Artru, M. Mekhfi, Z. Phys. **C 45** 669 (1990).
8. R.L. Jaffe, Phil. Trans. Roy. Soc. Lond. **A 359**, 391 (2001) [arXiv:hep-ph/0008038].
9. A. Freund, Phys. Lett. **B 472**, 412 (2000).
10. A. Freund, M. McDermott, Eur. Phys. J. **C 23**, 651 (2002).
11. A.V. Belitsky, D. Müller, A. Kirchner, Nucl. Phys. **B 629**, 323 (2002).
12. M. Diehl *et al.*, Phys. Lett **B 411**, 193 (1997).
13. HERMES coll., A. Airapetian *et al.*, Phys. Rev. Lett. **87**, 182001 (2001).
14. CLAS coll., S. Stepanyan *et al.*, Phys. Rev. Lett. **87**, 182002 (2001).
15. V.A. Korotkov, W.-D. Nowak, Nucl. Phys. **A 711**, 175 (2002) [arXiv:hep-ph/0207103].
16. F. Ellinghaus for the HERMES coll., Nucl. Phys. **A 711**, 171 (2002) [arXiv:hep-ex/0207029].
17. K. Goetze, M.V. Polyakov, M. Vanderhaeghen, Progr. Part. Nucl. Phys. **47**, 401 (2001).
18. X. Ji, W. Melnitchouk, X. Song, Phys. Rev. **D 56**, 5511 (1997).
19. HERMES coll., DESY PRC 01-01, 2002.
20. V.A. Korotkov, W.-D. Nowak, Eur. Phys. J. **C 23**, 455 (2002).
21. D.Yu. Ivanov *et al.*, CPHT RR 059.0602, arXiv:hep-ph/0209300.
22. A.V. Belitsky, D. Müller, Phys. Lett. **B 486**, 369 (2000).
23. P. Hoodbhoy, X. Ji, W. Lu, Phys. Rev. **D 59**, 014013 (1999).
24. Particle Data Group, D.E. Groom *et al.*, Eur. Phys. J. **C 15**, 1 (2000).
25. M. Beckmann for the HERMES coll., arXiv:hep-ex/0210049, to be publ. in Proc. of the ‘Workshop on Testing QCD through Spin Observables in Nuclear Targets’, Charlottesville, Virginia/USA, Apr. 18-20, 2002.
26. COMPASS coll., CERN/SPSLC 96-14 (1996).
27. V.A. Korotkov, W.-D. Nowak, K. Oganessyan, Eur. Phys. J. **C 18**, 639 (2001).
28. G. Bunce *et al.*, Ann. Rev. Nucl. Part. Sci. **50**, 525 (2000).
29. W.-D. Nowak, Nucl. Phys. **B** (Proc. Suppl.) **105**, 171 (2002).
30. R.L. Jaffe, MIT-CTP-2685, arXiv:hep-ph/9710465.
31. X. Ji, Proc. of the ‘15th Int. Spin Symposium’, Long Island, New York/USA, Sept. 9-14, 2002.
32. D.A. Demir, M. Pospelov, A. Ritz, arXiv:hep-ph/0208257.
33. S. Aoki *et al.*, Phys. Rev. **D 56**, 433 (1997).
34. S. Capitani *et al.*, Nucl. Phys. **B** (Proc. Suppl.) **79**, 548 (1999).
35. R. Altmeyer *et al.*, Phys. Rev. **D 49**, 3087 (1994).
36. B.W. Filippone, X. Ji, arXiv:hep-ph/0101224.
37. J.J. Kelly, these Proceedings and Proc. of the ‘15th Int. Spin Symposium’, Long Island, New York/USA, Sept. 9-14, 2002.
38. R. Kaiser, Proc. of the ‘15th Int. Spin Symposium’, Long Island, New York/USA, Sept. 9-14, 2002.

## Major Physics Topics to Study the Hadron Structure at a High-luminosity Fixed-target eN-facility

Physics	Measured Functions	Processes	Experimental Requests				
			target	$\sigma$	t	$Q^2$	$E_{beam}$
<p style="color: red; margin: 0;"><b>EXCLUSIVE REACTIONS:</b></p> <ul style="list-style-type: none"> <li style="color: green; margin: 0;">• <u>Total quark angular momentum <math>J^q</math>*</u>  <math>J^q = \sum_f J^f</math>                      (→ Orbital quark ang. mom. <math>L^q</math>)</li> <li style="margin: 0;">1<sup>st</sup> step: <math>J^u</math> (2006 +)</li> </ul>	<p style="color: green; margin: 0;"><b>GPDs:</b> Ji's relation:  <math>J^f = \lim_{t \rightarrow 0} \int x dx \{ H^f(x, \xi, t) + E^f(x, \xi, t) \}</math></p> <p style="margin: 0;">1<sup>st</sup> extraction: <math>Im H</math> (&lt; 2006 ?)</p>	<p style="color: blue; margin: 0;"><b>DVCS:</b> <math>H, E, \tilde{H}, \tilde{E}</math></p> <p style="color: blue; margin: 0;"><b>DVEM:</b></p> <p style="color: blue; margin: 0;">pseudo-scalar: <math>\tilde{H}, \tilde{E}</math></p> <p style="color: blue; margin: 0;">vector: <math>H, E</math></p>	<p style="color: red; margin: 0;">U, T</p>	<p style="color: blue; margin: 0;">low <math>\sigma \rightarrow</math> high <math>\int \mathcal{L} dt</math></p>	<p style="color: red; margin: 0;">low t → recoil det.</p>	<p style="color: red; margin: 0;">1 ... 20 GeV<sup>2</sup></p>	<p style="color: red; margin: 0;">30 ... 100 GeV</p>
<p style="color: red; margin: 0;"><b>SEMI-INCLUSIVE DIS:</b></p> <ul style="list-style-type: none"> <li style="color: green; margin: 0;">• <u>PRECISE</u> Measurement of                      ⇒ tensor charge:                      (→ <u>chiral symmetry breaking</u>)*</li> <li style="margin: 0;">⇒ axial charge:</li> </ul>	<p style="color: red; margin: 0;">transversity distributions</p> <p style="color: red; margin: 0;"><math>\delta q_f(x, Q^2) \equiv h_1^f(x, Q^2) \equiv \Delta_T^f(x, Q^2)</math></p> <p style="color: red; margin: 0;"><math>\delta \Sigma(Q^2) = \sum_f \int dx \{ \delta q_f(x, Q^2) - \delta \bar{q}_f(x, Q^2) \}</math></p> <p style="color: red; margin: 0;"><math>\Delta \Sigma(Q^2) = \sum_f \int dx \{ \Delta q_f(x, Q^2) + \Delta \bar{q}_f(x, Q^2) \}</math></p>	<p style="color: red; margin: 0;"><b>SIDIS + DIS</b></p> <ul style="list-style-type: none"> <li style="color: red; margin: 0;">• eN → e' KX for access to <math>\delta s(x, Q^2)</math></li> </ul>	<p style="color: red; margin: 0;">T</p> <p style="color: red; margin: 0;">L</p>	<p style="color: blue; margin: 0;">→ high precision high <math>\int \mathcal{L} dt</math></p>	<p style="color: red; margin: 0;">don't care</p>	<p style="color: red; margin: 0;">1 ... 20 GeV<sup>2</sup></p>	<p style="color: red; margin: 0;">50 ... 200 GeV</p>

\*) fundamental issues !

Summary of requests:

- polarized solid-state targets (T,L);
  - sufficient duty cycle ( $\geq 10\%$ )
  - Variable beam energy (30 ... 200 GeV)
- }  $\int \mathcal{L} dt \geq 100 \text{ fb}^{-1}/\text{year}$

WDN/KP-Oct.2002

Figure 4. Table of major physics topics in conjunction with experimental requirements.